J. Am. Soc. Mass Spectrom. (2017) 28:2602–2613
DOI: 10.1007/s13361-017-1780-2

RESEARCH ARTICLE

Influence of Linkage Stereochemistry and Protecting Groups on Glycosidic Bond Stability of Sodium Cationized Glycosyl Phosphates

Y. Zhu, Zhihua Yang, M. T. Rodgers

Department of Chemistry, Wayne State University, Detroit, MI 48202, USA

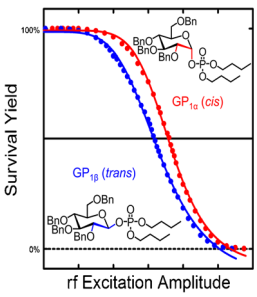

Abstract. Energy-resolved collision-induced dissociation (ER-CID) experiments of sodium cationized glycosyl phosphate complexes, $[GP_x+Na]^+$, are performed to elucidate the effects of linkage stereochemistry (α versus β), the geometry of the leaving groups (1,2-*cis* versus 1,2-*trans*), and protecting groups (cyclic versus non-cyclic) on the stability of the glycosyl phosphate linkage via survival yield analyses. A four parameter logistic dynamic fitting model is used to determine $CID_{50\%}$ values, which correspond to the level of rf excitation required to produce 50% dissociation of the precursor ion complexes. Present results suggest that dissociation of 1,2-*trans* $[GP_x+Na]^+$ occurs via a McLafferty-type rearrangement that is facilitated by a *syn* orientation of the leaving groups, whereas dissociation of 1,2-*cis* $[GP_x+Na]^+$ is more energetic as it involves the formation of an oxocarbenium ion intermediate. Thus, the C1–C2 configuration plays a major role in determining the stability/reactivity of glycosyl phosphate stereoisomers. For 1,2-*cis* anomers, the cyclic protecting groups at the C4 and C6 positions stabilize the glycosidic bond, whereas for 1,2-*trans* anomers, the cyclic protecting groups at the C4 and C6 positions tend to activate the glycosidic bond. The C3 *O*-benzyl (3 BnO) substituent is key to determining whether the sugar or phosphate moiety retains the sodium cation upon CID. For 1,2-*cis* anomers, the 3 BnO substituent weakens the glycosidic bond, whereas for 1,2-*trans* anomers, the 3 BnO substituent stabilizes the glycosidic bond. The C2 *O*-benzyl substituent does not significantly impact the glycosidic bond stability regardless of its orientation.

Keywords: Anomers, Energy-resolved collision-induced dissociation, Glycosyl phosphates, Mass spectrometry, Sodium cationization, Survival yield analysis

Received: 29 March 2017/Revised: 5 August 2017/Accepted: 8 August 2017/Published Online: 18 September 2017

Introduction

Oligosaccharides are involved in many biological processes, such as inflammation, immune response, and viral infections [1, 2]. In addition, functional oligosaccharides show positive effects on human health, both in the prevention and treatment of chronic diseases [3]. A variety of approaches for oligosaccharide synthesis have been reported that include: solid-phase based synthesis [4], the one-step synthesis [5], the two-stage activation procedure [6], enzyme assisted synthesis [7], and the one-pot sequential synthesis [8]. Among these strategies, the one-pot sequential synthesis is advantageous because it can be used to synthesize oligosaccharide libraries very efficiently with automated control [9]. This approach integrates several glycosylation steps into a single synthetic operation based on the differences of reactivity of various glycosyl donors. Glycosyl donors are sequentially added to the reaction system in the order of reduced reactivity (most reactive first), until the least reactive glycosyl donor is placed at the reducing end [9–11]. Glycosyl phosphates play important roles in oligosaccharide synthesis as they serve as great glycosyl donor because the phosphate moiety is an excellent leaving group [12, 13]. Therefore, it is very interesting to understand the effects of linkage stereochemistry, the geometry of the leaving groups, and protecting groups on the stability of the glycosyl phosphate linkage so that more effective glycosyl donors can be developed and synthesized.

The study of carbohydrate biology has seen enormous growth in the past decade, and as a result, there is an increasing need for improved analytical characterization [14–17]. Mass

Electronic supplementary material The online version of this article (https://doi.org/10.1007/s13361-017-1780-2) contains supplementary material, which is available to authorized users.

Correspondence to: M. T. Rodgers; *e-mail:* mrodgers@chem.wayne.edu

spectrometry has been used to effectively distinguish glycosyl phosphate (GP_x) isomers and offers the possibility of examining details of their reactivity/stability. The influence of linkage stereochemistry, leaving group geometry, and protecting groups on the stability of a series of GP_x has been evaluated by in-source threshold fragmentation electrospray ionization (ESI) mass spectrometry (MS) of the sodium cationized complexes of these GP_x [18]. However, in-source fragmentation of $[GP_x+Na]^+$ is influenced by many factors, including spray conditions, analyte concentration, and pH. Moreover, the fragment ions observed are typically accompanied by product ions derived from glycosylation and/or hydrolysis that occurs in solution. Thus, results are not generally interpreted straightforwardly.

Collision-induced dissociation (CID) is a powerful activation method commonly employed in mass spectrometry analyses to elucidate structural information, including isomer differentiation and characterization of ion fragmentation behavior and mechanisms [19]. In the case of carbohydrates, CID offers the possibility to assign details of carbohydrate structure such as sugar sequence and linkage positions [20–27]. McLafferty rearrangements are common molecular rearrangement reactions observed in mass spectrometry [28]. In the case of carbohydrates, most of the observed glycan rearrangements appear to be linked to the presence of a proton [29]. However, McLafferty-type, even-electron rearrangements have been observed for both deprotonated and metal cationized systems [30, 31]. Indeed alkali metal cationization has been widely used to characterize structure and investigate the CID behavior of carbohydrates [32–35]. The choice of alkali metal cation does influence the CID behavior. The smaller alkali metal cations (i.e., Li^+ and Na^+) are generally chosen as they bind more tightly and produce richer CID mass spectra, which facilitate structural elucidation and isomer differentiation [36–41]. The larger alkali metal cations often bind to carbohydrates weakly enough that only simple noncovalent bond cleavage occurs such that their CID provides almost no direct structural information [42, 43]. As isomeric carbohydrate complexes generally exhibit highly parallel fragmentation pathways, the energy dependence of the CID behavior has been found to provide additional information that is often key to their differentiation [44–46]. CID-based survival yield analysis was initially developed as a tool to quantify the distribution of precursor ion internal energies to explain fragmentation patterns that are observed in tandem mass spectrometry experiments [47, 48]. Survival yield analysis has since been used as a method to correlate conditions in the mass spectrometer to the energetics of sample ions. These studies have developed energy-dependent models for understanding molecular decompositions that occur upon CID [49–51].

Recently, survival yield analyses have been used to examine and compare the energetics of dissociation for noncovalently bound complexes as well as to the activated cleavage of covalent bonds. In particular, survival yield analyses have been employed to examine the disruption of noncovalent interactions of macrocyclic polyethers with alkali metal cations [52], ligand binding modes to duplex and triplex DNA [53], the analysis and structural differentiation of seven isomers with the chemical formula $C_9H_{11}NO_2$ [49], and have also been used to determine the relative *N*-glycosidic bond stabilities of protonated and sodium cationized DNA and RNA nucleosides [54–58]. Correlation between collision energy and dissociation of precursor ions has been semi-quantified in terms of EC50 or $CID_{50\%}$, the rf excitation energy (voltage) that results in 50% dissociation of the precursor ion [49, 52–60].

In this study, we investigate the stability of a series of sodium cationized glycosyl phosphates, $[GP_x+Na]^+$, via survival yield analyses based on their energy-resolved collision-induced dissociation (ER-CID) behavior. The GP_x examined are shown in Figure 1. $GP_{1\alpha}$ and $GP_{1\beta}$ are 2,3,4,6-tetra-*O*-benzyl-α- and β-D-glucosyl dibutyl phosphate, respectively, which are isomers with the chemical formula $C_{42}H_{53}O_9P$. $GP_{2\alpha}$ and $GP_{2\beta}$ are 2-*O*-benzyl-4,6-O-benzylidene-α- and β-D-glucosyl dibutyl phosphate, respectively, which are isomers with the chemical formula $C_{28}H_{39}O_8P$ and carry a 4,6-*O*-benzylidene acetyl cyclic protecting group, but lack a 3-*O*-benzyl substituent. For convenient comparison, $GP_{3\alpha}$ and $GP_{3\beta}$ are used to represent 2,3-di-*O*-benzyl-4,6-O-benzylidene-α- and β-D-mannopyranosyl dibutyl phosphate, respectively, whereas $GP_{4\alpha}$ and $GP_{4\beta}$ are 2,3-di-*O*-benzyl-4,6-O-benzylidene-α- and β-D-glucosyl dibutyl phosphate, respectively. $GP_{3\alpha}$, $GP_{3\beta}$, $GP_{4\alpha}$, and $GP_{4\beta}$ are isomers with the chemical formula $C_{35}H_{45}O_9P$, which carry the same 4,6-*O*-benzylidene acetyl cyclic protecting group as $GP_{2\alpha}$ and $GP_{2\beta}$. A four parameter logistic dynamic fitting model is employed to extract $CID_{50\%}$ values. Trends in the $CID_{50\%}$ values are examined to elucidate the effects of linkage stereochemistry, the geometry of the leaving group, and protecting groups on the stability of the glycosyl phosphate linkage and thus the efficiency of these species to serve as glycosyl donors for carbohydrate synthesis, and are found to provide insight into the mechanism by which these sodium cationized GP_x complexes dissociate.

Experimental Procedure and Survival Yield Analysis

Chemicals

The eight glycosyl and mannopyranosyl dibutyl phosphates used in this work were synthesized using synthetic procedures described previously [61–64]. Methanol (MeOH, HPLC grade) was purchased from EMD Millipore Co., Billerica, MA, USA. DI water (HPLC grade) was purchased from EMD Chemicals Inc., Gibbstown, NJ, USA. Sodium acetate (NaOAc) was purchase from Sigma-Aldrich, St. Louis, MO, USA.

Mass Spectrometry

ER-CID experiments of sodium cationized GP_x were performed using a Bruker amaZon ETD quadrupole ion trap mass

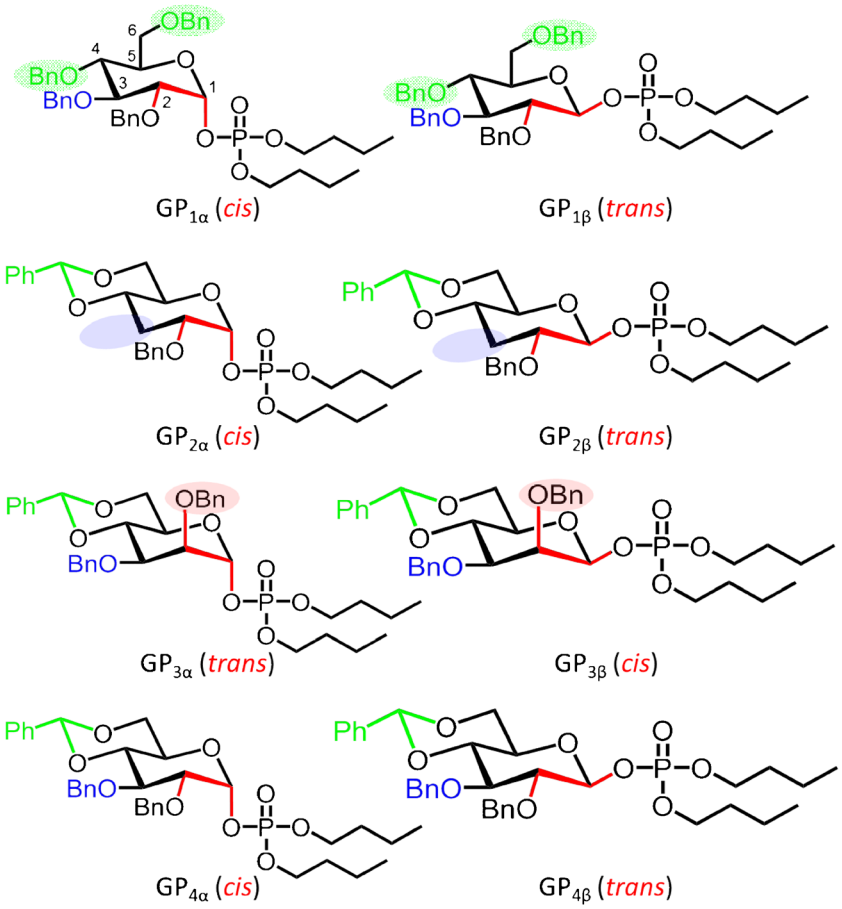

Figure 1. Structures of the eight glycosyl phosphates (GP_x) examined in this work, $GP_{1\alpha}$, $GP_{1\beta}$, $GP_{2\alpha}$, $GP_{2\beta}$, $GP_{3\alpha}$, $GP_{3\beta}$, $GP_{4\alpha}$, and $GP_{4\beta}$. The GP_α versus GP_β isomers differ only in the C1-C2 configuration, *cis* versus *trans*. $GP_{1\alpha}$ and $GP_{1\beta}$, possess two *O*-benzyl substituents (at C4 and C6) rather than a cyclic protecting group, $GP_{2\alpha}$ and $GP_{2\beta}$ instead lack a 3 BnO substituent, whereas the 2 BnO substituent of $GP_{3\alpha}$ and $GP_{3\beta}$ is axial rather than equatorial, as highlighted in the figure

spectrometer (QIT MS) (Bruker Daltonics, Bremen, Germany). Sample solutions were prepared by dissolving the GP_x in a 50%:50% MeOH:H_2O solution to a concentration of ~10 μM to which a sodium acetate solution was then added to produce a final concentration of 0.1 mM NaOAc for direct infusion electrospray ionization (ESI). The sodium cationized GP_x complexes were generated using an Apollo ESI source at a flow rate of 3 μL/min. The N_2 drying gas temperature was set at 200 °C and a flow rate of 3 L/min. The N_2 nebulizer gas was set at 0.69 bar. The ESI probe capillary voltage was set at −4.5 kV with the end plate offset set at −500 V. Helium was used as the cooling and collision gas at a stagnation pressure in the ion trap of ~1 mTorr. The number of trapped ions was kept constant (2×10^5) using the ion charge control (ICC) in all experiments. The low-mass cutoff for the ER-CID experiments was set to 27%, corresponding to a q_z value of 0.25. The rf excitation amplitude was varied from 0 V to the amplitude required to produce complete fragmentation of the precursor glycosyl phosphate complex at a step size of 0.01 V. An activation time of 40 ms was used for all CID experiments. Data analysis was performed using Compass Data Analysis 4.0 software (Bruker Daltonics, Bremen, Germany).

Survival Yield Analysis

Survival yield analysis is a robust technique to study the relative stabilities of various ions when judiciously applied [65–68]. In order to elucidate the relative stabilities of eight $[GP_x+Na]^+$ complexes, survival yield analyses of these complexes were performed by calculating and comparing the survival yields based on the ER-CID experimental results as a function of rf excitation amplitude. The survival yield of each $[GP_x+Na]^+$ complex was determined based on the ratio of the intensity of the precursor glycosyl phosphate complex (I_p) to the total ion intensity as shown in Equation 1,

$$Survival\ \ yield = I_p / \left(I_p + \sum_i I_{f_i} \right) \quad (1)$$

where $\sum_i I_{f_i}$ is the total fragment ion intensity. The survival yield of $[GP_x+Na]^+$ was plotted as a function of rf excitation amplitude to generate the survival yield curve. The $CID_{50\%}$ value, which represents the rf excitation amplitude required to produce 50% dissociation of precursor glycosyl phosphate

complex was determined by four parameter logistic dynamic fitting as shown in Equation 2,

$$Survival\ \ Yield = \min + \frac{\max - \min}{1 + (rf_{EA}/CID_{50\%})^{CIDslope}} \quad (2)$$

where max and min are the maximum (1) and minimum (0) values of the survival yield, rf_{EA} is the rf excitation amplitude applied, and CIDslope is the slope of the declining region of the survival yield curve. Because the fragmentation of the $[GP_x+Na]^+$ complexes is dominated by glycosidic bond cleavage, the $CID_{50\%}$ values of $[GP_x+Na]^+$ provide the relative glycosidic bond stabilities of these complexes. Data analysis was performed using SigmaPlot 10.0 (Systat Software, Inc., San Jose, CA, USA).

Results

CID Fragmentation Pathways of $[GP_x+Na]^+$

The CID mass spectra of eight sodium cationized GP_x at an rf excitation amplitude that results in approximately 50% dissociation are compared in Figure 2. The *m/z* values of the precursor $[GP_x+Na]^+$ complexes and their CID products are given in the figure and summarized in Supplementary Table S1 in the Electronic Supplementary Material, whereas survival/fragment yields for each $[GP_x+Na]^+$ complex across the entire range of rf_{EA} values measured are shown in Supplementary Figure S1. For all eight sodium cationized glycosyl phosphates examined, the primary fragmentation pathway across the entire range of rf_{EA} values observed involves cleavage of the glycosidic bond with the sodium cation retained by either the sugar or phosphate moieties as summarized in the Reactions 3 and 4, respectively (see Supplementary Figure S1).

$$[GP_x+Na]^+ \xrightarrow{n\ He} [GP_x-DBPA+Na]^+ + DBPA \quad (3)$$

$$[GP_x+Na]^+ \xrightarrow{n\ He} [DBPA+Na]^+ + (GP_x-DBPA) \quad (4)$$

Reaction 3 is the primary CID pathway for the $[GP_x+Na]^+$ complexes of $GP_{1\alpha}$, $GP_{1\beta}$, $GP_{3\alpha}$, $GP_{3\beta}$, $GP_{4\alpha}$, and $GP_{4\beta}$ and observed as a loss of 210 Da (●) from the precursor glycosyl phosphate complex (loss of DBPA) as the sodium cation is preferentially retained by the sugar moiety. In contrast, loss of neutral DBPA from $[GP_{2\alpha}+Na]^+$ and $[GP_{2\beta}+Na]^+$ is only a very minor dissociation pathway. Instead the dibutyl phosphoric acid moiety preferentially retains the sodium cation upon CID of the $[GP_{2\alpha}+Na]^+$ and $[GP_{2\beta}+Na]^+$ complexes, Reaction 4 (●). Reaction 4 is also a minor CID pathway for $GP_{3\alpha}$, $GP_{3\beta}$, $GP_{4\alpha}$, and $GP_{4\beta}$ at elevated values of rf_{EA}. It should be noted that $GP_{1\alpha}$, $GP_{1\beta}$, $GP_{3\alpha}$, $GP_{3\beta}$, $GP_{4\alpha}$, and $GP_{4\beta}$ all possess a 3-*O*-benzyl protecting group, whereas both $GP_{2\alpha}$ and $GP_{2\beta}$ possess neither a 3-hydroxyl substituent nor a 3-*O*-benzyl protecting group, suggesting that the configuration at the C3 position plays a key role in determining which fragment retains the sodium cation upon dissociation of the glycosidic bond.

Sequential dissociation of the sodium cationized glycoside, ($[GP_x-DBPA+Na]^+$, (●) resulting in a further loss of 91 Da, is also observed in the CID of sodium cationized $GP_{1\alpha}$, $GP_{1\beta}$, $GP_{3\alpha}$, $GP_{3\beta}$, $GP_{4\alpha}$, and $GP_{4\beta}$, Reaction 5 (●), and is the most abundant minor product observed for these complexes (see Supplementary Figure S1). This may be deduced as a loss of one of the benzyl protecting groups (Bn) as a tropylium radical.

$$[GP_x+Na]^+ \xrightarrow{n\ He} [GP_x-DBPA-Bn+Na]^+ + DBPA + Bn \quad (5)$$

$GP_{1\alpha}$ and $GP_{1\beta}$ uniquely exhibit two minor fragmentation pathways that involve loss of 90 Da from the ionic product of Reaction (3) and 420 Da from the precursor complex, Reactions 6 (●) and 7 (●). The loss of 90 Da likely involves elimination of C_7H_6. However, the 420 Da loss pathway is not obviously assigned, but does correspond to a mass loss equivalent to that of four benzyl protecting groups and butene (4Bn+B).

$$[GP_x+Na]^+ \xrightarrow{n\ He} [GP_x-DBPA-C_7H_6+Na]^+ + DBPA + C_7H_6 \quad (6)$$

$$[GP_x+Na]^+ \xrightarrow{n\ He} [GP_x-4Bn-B+Na]^+ + 4Bn + B \quad (7)$$

At elevated rf excitation amplitudes, another minor dissociation pathway involving the loss of 56 Da, and corresponding to loss of butene (B) is observed in the CID of the $GP_{2\alpha}$, $GP_{3\beta}$, and $GP_{4\alpha}$ complexes, Reaction 8 (●). Loss of 136 Da, corresponding to loss of monobutyl phosphoric acid (MBPA), is also observed as a minor dissociation pathway in the CID of the $GP_{1\alpha}$, $GP_{1\beta}$, $GP_{3\beta}$, and $GP_{4\alpha}$ complexes, Reaction 9 (●)

$$[GP_x+Na]^+ \xrightarrow{n\ He} [GP_x-B+Na]^+ + B \quad (8)$$

$$[GP_x+Na]^+ \xrightarrow{n\ He} [GP_x-MBPA+Na]^+ + MBPA \quad (9)$$

Elimination of PhCH=O (neutral loss of 106 Da) is observed as minor CID product for $GP_{2\alpha}$, $GP_{2\beta}$, and $GP_{4\alpha}$ at high rf_{EA} values, Reaction 10 (●).

$$[GP_x+Na]^+ \xrightarrow{n\ He} [GP_x-PhCH=O+Na]^+ + PhCH=O \quad (10)$$

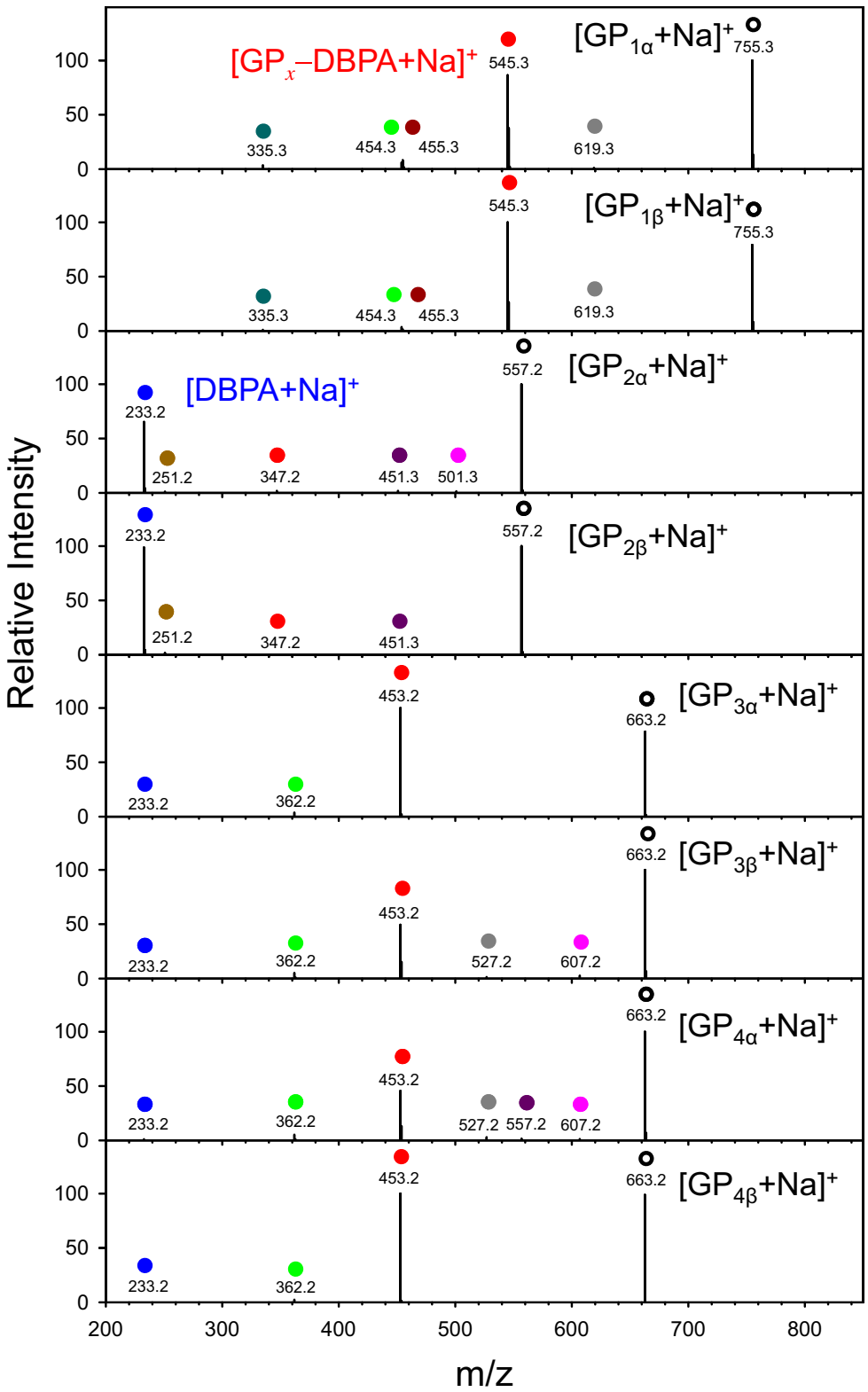

Figure 2. Energy-resolved CID mass spectra of eight sodium cationized glycosyl phosphates $[GP_x+Na]^+$, where x = 1α, 1β, 2α, 2β, 3α, 3β, 4α, and 4β. The precursor ion, $[GP_x+Na]^+$ is indicated by (○). The major CID product ions result from cleavage of the glycosyl phosphate linkage with the sodium cation retained by the sugar moiety corresponding to loss of 210 Da from the precursor ion $[GP_x–DBPA+Na]^+$ (reaction 3, ●), or retained by the phosphate moiety $[DBPA+Na]^+$, and observed at m/z = 233.2 Da (reaction 4, ●). Minor fragmentation pathways are also labeled with symbols with color coding as defined in the text for reactions (5)–(11)

The peak deduced as $[DBPA+W+Na]^+$ is only observed in the mass spectra of $GP_{2\alpha}$ and $GP_{2\beta}$, Reaction 11 (•). This product appears to be the result of adduction of a background water molecule (W) to the primary CID product $[DBPA+Na]^+$, which is stabilized by collisions with the He present in the trap.

$$[GP_x+Na]^+ \xrightarrow{n\ He} [DBPA+W+Na]^+ + (GP_x - DBPA - W) \quad (11)$$

Discussion

Mode of Sodium Cation Binding in the $[GP_x+Na]^+$ Complexes

Although the exact modes of sodium cation binding in the $[GP_x+Na]^+$ complexes are not known, the CID behavior observed suggests that Na^+ favorably binds to the sugar and phosphate moieties. What is not entirely clear is whether binding to both moieties occurs in the same conformer(s), or a mixture of conformers involving different modes of sodium cation binding are present in the experiments. All eight $[GP_x+Na]^+$ complexes exhibit Reaction 3 with the sodium cation preferentially retained by the sugar moiety for all but the complexes to $GP_{2\alpha}$ and $GP_{2\beta}$. Six of the $[GP_x+Na]^+$ complexes exhibit Reaction 4 with the sodium cation preferentially retained by the phosphate moiety only for $GP_{2\alpha}$ and $GP_{2\beta}$. These results clearly suggest that the 3 BnO substituent must be present and involved in the binding for the sodium cation to preferentially retain the sugar moiety upon CID. Given the geometry of these GP_x it seems unlikely that the mode of Na^+ binding could simultaneously involve both the phosphate moiety and the 3 BnO substituent, thus suggesting that a mixture of conformers involving two different modes of sodium cation binding (one involving the phosphate moiety with possible additional chelation interactions with the sugar, and another involving only chelation interactions with the sugar) are present for all complexes except those of $GP_{1\alpha}$ and $GP_{1\beta}$. Reaction 4 is not observed for $GP_{1\alpha}$ and $GP_{1\beta}$, suggesting that the 4- and 6-BnO substituents also contribute to enhanced binding to the sugar moiety, and do so more effectively than the cyclic protecting group, such that binding to the phosphate moiety is not competitive for these species. Numerous studies in the literature have found that sodium cations preferentially bind via multiple chelation interactions to hetero atoms [54–58, 69–73], and in particular oxygen atoms, and π-systems of organic and biologically relevant ligands [73–80]. Thus, the sugar moiety of each of these glycosyl phosphates offers multiple oxygen and π-donors for binding, whereas the phosphate moiety offers the oxo and alkoxy oxygen atoms for binding. Therefore, a mixture of conformers bound via multiple chelation interactions with the oxygen and π donors of the sugar moiety may be of similar stability and present in the experiments for $GP_{1\alpha}$, $GP_{1\beta}$, $GP_{3\alpha}$, $GP_{3\beta}$, $GP_{4\alpha}$, and $GP_{4\beta}$. A very minor population of phosphate bound species appears to be present for these complexes. For the complexes to $GP_{2\alpha}$ and $GP_{2\beta}$, it appears that binding to the phosphate moiety is preferred and likely involves the phosphate oxo oxygen, one or possibly two of the alkoxy oxygen atoms [73], and possibly the oxygen atom of the sugar ring.

Survival Yield Analyses of $[GP_x+Na]^+$

Effects of C1-C2 Configuration, Cis versus Trans Survival yield curves of the eight $[GP_x+Na]^+$ complexes are compared in Figure 3. Each anomeric pair is individually compared in parts a–d to readily elucidate the effects of the C1−C2 configuration on the stability of the glycosyl phosphate linkage. It should be noted that the GP_α exhibit a *cis* configuration at C1–C2 and the GP_β exhibit a *trans* configuration at C1–C2 for all GP_x except $GP_{3\alpha}$ and $GP_{3\beta}$ where the opposite is true. The $CID_{50\%}$ values of these complexes determined by four parameter logistic dynamic fitting are shown in Figure 3 and listed in Table 1 for comparison. Because the major fragmentation pathway observed in all cases involves glycosidic bond cleavage and accounts for >95% of the observed dissociation at all values of rf_{EA}, the $CID_{50\%}$ values provide a measure of the relative glycosidic bond stabilities. Overall, the $CID_{50\%}$ values of the 1,2-*cis* $[GP_x+Na]^+$ exceed those of the 1,2-*trans* $[GP_x+Na]^+$, indicating that the glycosidic bonds of 1,2-*cis* $[GP_x+Na]^+$ are more stable than those of the 1,2-*trans* $[GP_x+Na]^+$. Differences in the $CID_{50\%}$ values for the 1,2-*cis* and 1,2-*trans* anomeric pairs are smallest for $GP_{1\alpha}$ and $GP_{1\beta}$, which lack a cyclic protection group (0.064 V). Absence of the C3 BnO substituent also leads to a relatively small difference in the $CID_{50\%}$ values (0.094 V) for the 1,2-*cis* versus 1,2-*trans* isomers. In contrast, larger differences in the $CID_{50\%}$ values for the 1,2-*cis* versus 1,2-*trans* isomers are observed when both a cyclic protecting group and C3 BnO substituent are present, with a larger difference (0.324 V) found when the C2 BnO substituent is axial, and a somewhat smaller difference (0.310 V) when C2 BnO is equatorial. It has also been reported that it is the *trans* configuration between the substituents at C1–C2 and the resulting anchimeric assistance that controls the stereospecific CID behavior [14, 81, 82]. The present results clearly indicate that the C1–C2 configuration plays a major role in determining the stability/reactivity of glycosyl phosphate stereoisomers and that *syn* elimination from 1,2-*trans* $[GP_x+Na]^+$ is more favorable (less energetic) than *anti* elimination from 1,2-*cis* $[GP_x+Na]^+$. Although changes in the C1−C2 configuration alter the energetics for glycosidic bond cleavage, they do not alter the preferred reaction pathway for any of the isomeric pairs. Thus the mode of sodium cation does not appear to be significantly influenced by the C1−C2 configuration, which suggests that the C2 BnO substituent is likely not involved (or not a significant contributor) to the binding of the sodium cation.

D-Mannopyranosyl versus D-Glucosyl Dibutyl Phosphate Survival yield curves of the sodium cationized complexes of $GP_{3\alpha}$, $GP_{3\beta}$, $GP_{4\alpha}$, and $GP_{4\beta}$ are overlaid in Figure 4a. These

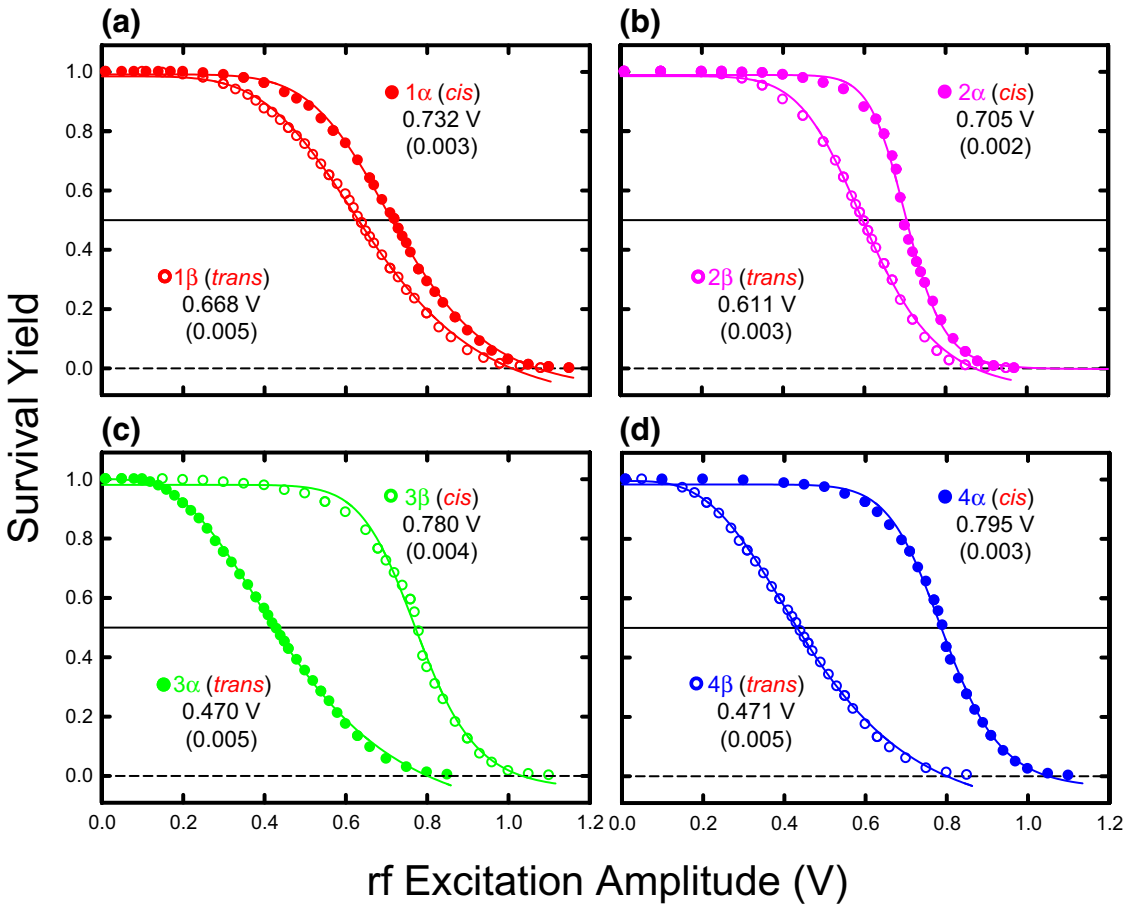

Figure 3. Survival yield curves for energy-resolved CID of eight sodium cationized glycosyl phosphates, $[GP_x+Na]^+$. Each anomeric pair is individually compared to facilitate elucidation of the effects of the C1-C2 linkage geometry and leaving group stereochemistry on the stability of the glycosyl phosphate linkage, (parts **a**–**d**)

GP_x are also anomeric pairs that differ only in the orientation of the C2 BnO substituent and C1−C2 configuration. The 1,2-*trans* isomers of these complexes exhibit very similar $CID_{50\%}$ values, whereas a modest change in the $CID_{50\%}$ values is observed for the 1,2-*cis* isomers. Thus, the orientation of the C2 BnO substituent exerts a negligible effect on the glycosidic bond stabilities of sodium cationized $GP_{3\alpha}$ and $GP_{4\beta}$, and a minor influence on those of $GP_{4\alpha}$ and $GP_{3\beta}$. In contrast, the C1–C2 configuration plays a major role in determining the stability/reactivity of glycosyl phosphate stereoisomers, consistent with the conclusion of the previous section.

Effects of the 3-O-Benzyl Substituent

The survival yield curves of the sodium cationized $GP_{2\alpha}$, $GP_{2\beta}$, $GP_{4\alpha}$, and $GP_{4\beta}$ are compared in Figure 4b. These complexes differ only in the absence or presence of the C3 BnO substituent

Table 1. Summary of the $CID_{50\%}$ Values of $[GP_x+Na]^+$ and Experimental Relative Abundances of Sodium Cationized Ions Formed Upon Glycosidic Bond Cleavage

	C1-C2 configuration	$CID_{50\%}$ (V) (mean ± SD)[α]	$[GP_x–DBPA+Na]^+$	$[DBPA+Na]^+$
$GP_{1\alpha}$	*cis*	0.732 ± 0.003	major	not observed
$GP_{1\beta}$	*trans*	0.668 ± 0.005	major	not observed
$GP_{2\alpha}$	*cis*	0.705 ± 0.002	minor	major
$GP_{2\beta}$	*trans*	0.611 ± 0.003	minor	major
$GP_{3\alpha}$	*trans*	0.470 ± 0.005	major	minor
$GP_{3\beta}$	*cis*	0.780 ± 0.004	major	minor
$GP_{4\alpha}$	*cis*	0.795 ± 0.003	major	minor
$GP_{4\beta}$	*trans*	0.471 ± 0.005	major	minor

[α]SD = one standard deviation of the mean $CID_{50\%}$ value

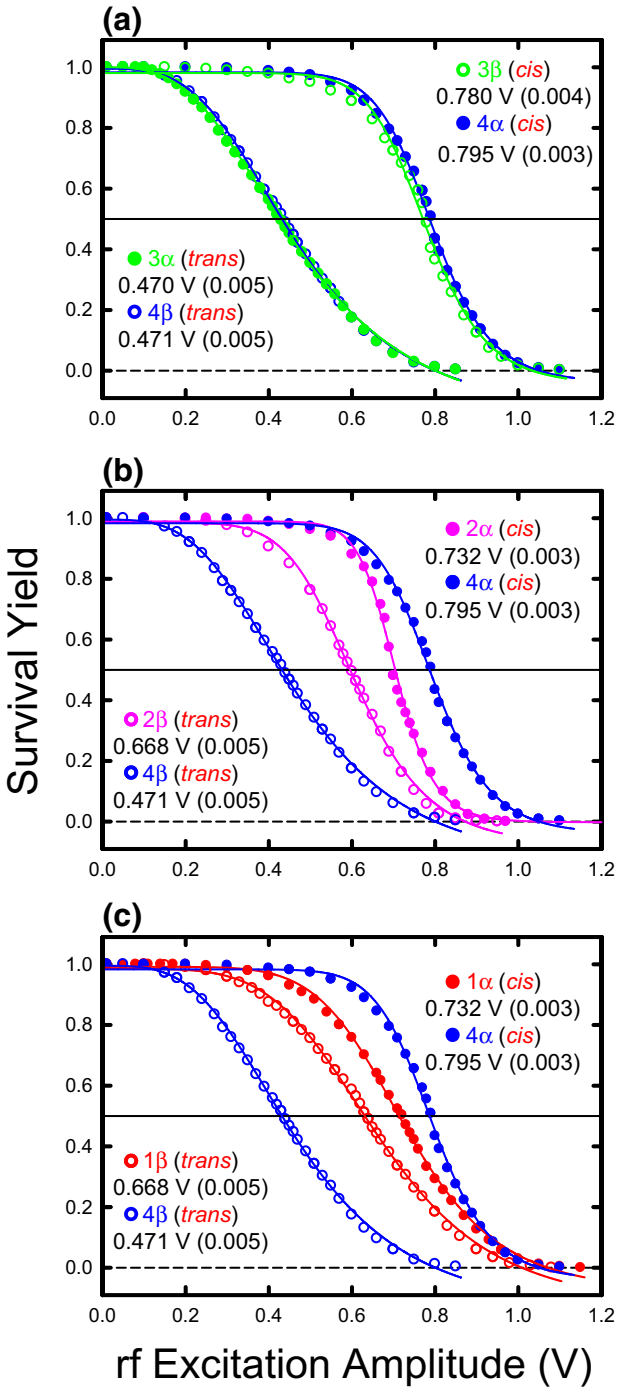

Figure 4. Survival yield curves for energy-resolved CID of eight sodium cationized glycosyl phosphates, $[GP_x+Na]^+$. Overlays of the survival yield curves of the anomeric pair $GP_{4\alpha}$ and $GP_{4\beta}$ with each of the other anomeric pairs are shown (parts **a**–**c**) are shown to facilitate elucidation of the effects of the orientation of the C2 BnO substituent ($GP_{3\alpha}$ and $GP_{3\beta}$), the presence of the C3 BnO substituent ($GP_{2\alpha}$ and $GP_{2\beta}$), and the cyclic protecting group ($GP_{1\alpha}$ and $GP_{1\beta}$) on the glycosidic bond stabilities of these complexes

and the C1−C2 configuration. As discussed above, the C3 BnO substituent is key to determining whether the sugar or phosphate moiety retains the sodium cation upon CID. As can be seen in the figure, the C3 BnO substituent has a more significant effect on the dissociation energetics of the 1,2-*trans* (lowers the activation barrier) than the 1,2-*cis* complexes (increases the activation barrier). Thus, the 3-*O*-benzyl substituent is critical to the mode of binding, whereas its influence on glycosidic bond stability depends on the C1−C2 configuration.

Effects of Cyclic Protecting Groups

The survival yield curves of sodium cationized $GP_{1\alpha}$, $GP_{1\beta}$, $GP_{4\alpha}$, and $GP_{4\beta}$ are compared in Figure 4c to elucidate the effect of the cyclic protecting group at the C4 and C6 positions on the glycosidic bond stabilities of $[GP_x+Na]^+$. These complexes are chosen for comparison to examine the effects of the C4 and C6 BnO substituents of $GP_{1\alpha}$ and $GP_{1\beta}$ versus the cyclic protecting group at the C4 and C6 positions of $GP_{4\alpha}$ and $GP_{4\beta}$ on glycosidic bond stability. Previous studies using in-source fragmentation showed that a greater cone voltage is required to dissociate the glycosidic bonds of sodium cationized glycosyl phosphates that possess a cyclic protecting group [18]. Figure 4c shows that the sodium cationized forms of a 1,2-*cis* anomer carrying a cyclic protecting group, $[GP_{4\alpha}+Na]^+$ ($CID_{50\%}$ = 0.795 V), is more stable than $[GP_{1\alpha}+Na]^+$ (which does not possess a cyclic protecting group, $CID_{50\%}$ = 0.732 V), which suggests that the cyclic protecting group at the C4 and C6 enhances the stability of the anomer bearing a 1,2-*cis* configuration. This result is in agreement with the in-source threshold fragmentation studies [18]. For the sodium cationized forms of 1,2-*trans* isomers with a cyclic protecting group at the C4 and C6 positions, $[GP_{4\beta}+Na]^+$ ($CID_{50\%}$ = 0.471 V), are more active than that of $[GP_{1\beta}+Na]^+$ (which does not possess a cyclic protecting group, $CID_{50\%}$ = 0.668 V). Thus the effect of the cyclic protecting group on glycosidic bond stability is also correlated with the C1−C2 configuration.

Effects of the Mode of Sodium Cation Binding

Although the exact modes of sodium cation binding in the $[GP_x+Na]^+$ complexes are not known, they do not appear to be significantly influenced by the C1−C2 configuration as the same dominant CID pathway is observed for each anomeric pair. Instead, the C3 BnO substituent appears to be key to determining the preferred mode of sodium cation binding. For the complexes of $GP_{1\alpha}$, $GP_{1\beta}$, $GP_{3\alpha}$, $GP_{3\beta}$, $GP_{4\alpha}$, and $GP_{4\beta}$, the cation binds to the sugar moiety such that the sodium cation is remote from the glycosidic bond cleavage process. Thus, the sodium cation is not expected to exert a significant impact of the dissociation energetics, and primarily serves as a charge carrier to enable this reaction to be observed mass spectrometrically. In contrast, for the complexes of $GP_{2\alpha}$ and $GP_{2\beta}$, where binding involves the phosphate moiety, it appears that binding of the sodium cation activates the glycosidic bond of the 1,2-*cis* isomer and stabilizes the glycosidic bond of the 1,2-*trans* isomer. This is consistent with expectations based on the mechanisms proposed below and will be revisited in the mechanistic discussion of the next section.

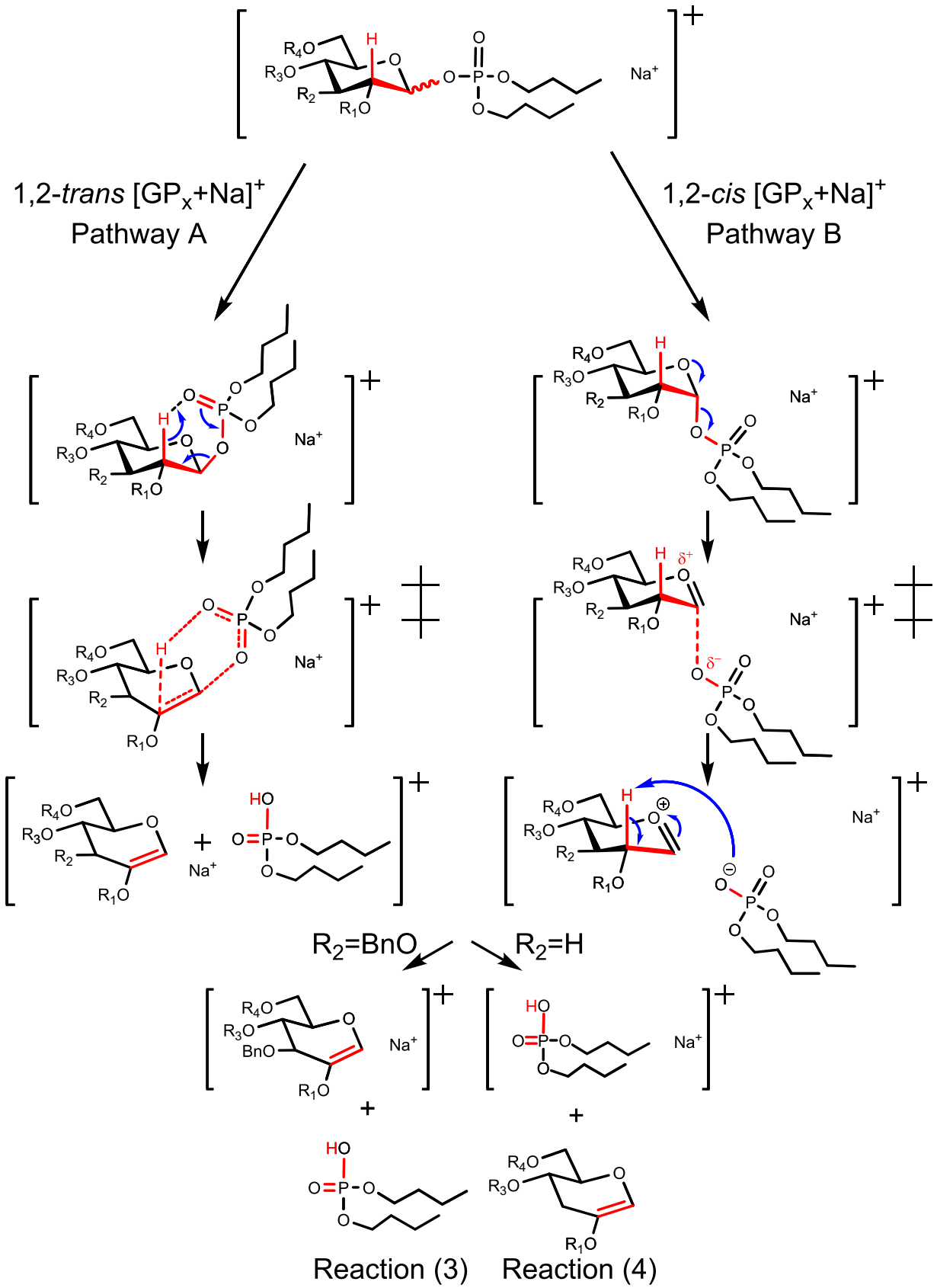

Figure 5. Proposed mechanisms for glycosidic bond cleavage of 1,2-*trans* and 1,2-*cis* sodium cationized glycosyl phosphates, $[GP_x+Na]^+$

Mechanism of Glycosidic Bond Cleavage

The lower $CID_{50\%}$ values determined for 1,2-*trans* $[GP_x+Na]^+$ suggest that a plausible mechanism for cleavage of the glycosidic bond involves *syn* elimination via a McLafferty-type rearrangement as shown in Figure 5 pathway A for anomers bearing a *trans* configuration at C1–C2. During the unimolecular dissociation process, based on a McLafferty-type rearrangement, H2 is transferred to the dibutyl phosphate moiety via a six-membered ring transition state, which leads to the loss of neutral dibutyl phosphoric acid. When R_2 = BnO, the substituent is involved in the binding and provides an additional chelation interaction with the sodium cation. Therefore, neutral dibutyl phosphoric acid loss becomes the dominant fragmentation pathway observed for anomers of GP_1, GP_3, and GP_4 (reaction 3, ●). When R_2 = H, the absence of the C3 BnO substituent leads to preferential binding to the phosphate moiety, and thus sodium cationized dibutyl phosphoric acid, $[DBPA+Na]^+$, becomes the dominant ionic product observed for both GP_2 anomers (Reaction 4, ●). The fragmentation of 1,2-*cis* anomers likely involves the formation of an oxocarbenium ion intermediate as shown in Figure 5 pathway B [18]. The formation of an oxocarbenium ion transition state has been assumed as the rate-determining step of the one-pot sequential synthesis [9, 18]. Elongation of the glycosidic bond leads to formation of an oxocarbenium ion intermediate. Transfer of the H2 atom to the dibutyl phosphate moiety then produces the observed products. The ability of the 1,2-*cis* anomers to stabilize the transition state for dissociation via hydrogen bonding in the six-membered ring formed reduces the activation energy relative to the 1,2-*trans* anomers, consistent with the results of the survival yield analyses that find pathway B requires more energy than pathway A in the gas phase. Likewise, binding of Na^+ to the phosphate moiety would stabilize the oxocarbenium ion transition state (TS) of the 1,2-*cis* anomers and activate the glycosidic bond, whereas Na^+ binding to the phosphate moiety should weaken the hydrogen-bonding interaction and destabilize the TS for 1,2-*trans* species in accord with the experimental observations..

$CID_{50\%}$ versus Dissociation Onsets

The trends in the $CID_{50\%}$ values extracted from the ER-CID measurements performed here are used to assess the relative glycosidic bond stabilities of eight $[GP_x+Na]^+$ complexes. However, one might arbitrarily chose a different level of dissociation to make these assessments. Most often, the threshold or onset energy (or rf excitation energy) would be of interest. A detailed examination of Supplementary Figure S1 shows that 1,2-*trans* $[GP_x+Na]^+$ isomers begin to undergo glycosidic bond cleavage at lower values of the rf excitation energy than the corresponding 1,2-*cis* isomers, consistent with the trends in the $CID_{50\%}$ values. Likewise, the dissociation behavior of $GP_{3\alpha}$ versus $GP_{4\beta}$ and $GP_{3\beta}$ versus $GP_{4\alpha}$ are highly parallel over the entire range of excitation energies whether examining the survival yields of Figure 4 or the product yields of Supplementary Figure S1. Analogous comparisons hold for GP_{4x} versus GP_{2x} and GP_{1x} such that the value chosen for comparison is somewhat arbitrary for the $[GP_x+Na]^+$ complexes examined here.

Conclusions

The relative glycosidic bond stabilities of eight $[GP_x+Na]^+$ complexes have been examined via survival yield analyses based on ER-CID experiments performed in a QIT MS. Present results indicate that the C1-C2 configuration is a dominant factor influencing the stability of glycosyl phosphate linkage, such that 1,2-*cis* isomers, corresponding to a *trans* orientation of the leaving groups, are found to be more stable than the corresponding 1,2-*trans* isomers where the leaving groups are *syn*. Thus, the glycosyl phosphates having the leaving groups in a *syn* orientation (the 1,2-*trans* isomers) make better glycosyl donors than those with the leaving groups *anti* (the 1,2-*cis* isomers). These behaviors suggest that a plausible mechanism for the glycosidic bond cleavage of 1,2-*trans* $[GP_x+Na]^+$ involves *syn* elimination via a McLafferty-type rearrangement, whereas the dissociation of 1,2-*cis* $[GP_x+Na]^+$ likely involves the formation of an oxocarbenium ion intermediate. The fragmentation behaviors indicate that the cyclic protecting groups stabilize the glycosidic bond of the 1,2-*cis* anomers, but is activating for the 1,2-*trans* anomers. The fragmentation behaviors also suggest that the C3 BnO substituent provides additional stabilization to the sodium cation, alters the fragment that retains Na^+ upon dissociation, and leads to the loss of neutral dibutyl phosphoric acid, Reaction 3 (●). The corresponding GP_3 and GP_4 complexes exhibit similar $CID_{50\%}$ values, suggesting that the orientation of the C2 BnO substituent does not significantly impact the glycosidic bond stabilities.

Acknowledgments

Financial support for this work was provided by the National Science Foundation Grant DBI-0922819 (for the Bruker amaZon ETD QIT MS employed in this work). Y. Zhu gratefully acknowledges support from a Wayne State University Thomas C. Rumble Graduate Fellowship. Z. Yang gratefully acknowledges Wayne State University Postdoctoral Grant Program. Thanks to W.-w. Chen and D. Crich for providing the glycosyl phosphates examined in this work.

References

1. Ryan, C.A.: Oligosaccharide signals: from plant defense to parasite offense. Proc. Natl. Acad. Sci. U. S. A. **91**, 1–2 (1994)
2. Zhang, Z.Y., Ollmann, I.R., Ye, X.S., Wischnat, R., Baasov, T., Wong, C.H.: Programmable one-pot oligosaccharide synthesis. J. Am. Chem. Soc. **121**, 734–753 (1999)
3. Xu, Q., Chao, Y.L., Wan, Q.B.: Health benefit application of functional oligosaccharides. Carbohydr. Polym. **77**, 435–441 (2009)
4. Danishefsky, S.J., Mcclure, K.F., Randolph, J.T., Ruggeri, R.B.: A strategy for the solid-phase synthesis of oligosaccharides. Science. **260**, 1307–1309 (1993)
5. Raghavan, S., Kahne, D.: A one-step synthesis of the ciclamycin trisaccharide. J. Am. Chem. Soc. **115**, 1580–1581 (1993)
6. Nicolaou, K.C., Dolle, R.E., Papahatjis, D.P., Randall, J.L.: Practical synthesis of oligosaccharides: partial synthesis of avermectin-B1a. J. Am. Chem. Soc. **106**, 4189–4192 (1984)
7. Ichikawa, Y., Shen, G.J., Wong, C.H.: Enzyme-catalyzed synthesis of sialyl oligosaccharide with insitu regeneration of CMP-sialic acid. J. Am. Chem. Soc. **113**, 4698–4700 (1991)
8. Yamada, H., Harada, T., Miyazaki, H., Takahashi, T.: One-pot sequential glycosylation – a new method for the synthesis of oligosaccharides. Tetrahedron Lett. **35**, 3979–3982 (1994)
9. Wang, Y.H., Ye, X.S., Zhang, L.H.: Oligosaccharide assembly by one-pot multi-step strategy. Org. Biomol. Chem. **5**, 2189–2200 (2007)
10. Ye, X.S., Wong, C.H.: Anomeric reactivity-based one-pot oligosaccharide synthesis: A rapid route to oligosaccharide libraries. J. Organomet. Chem. **65**, 2410–2431 (2000)
11. Wang, Z., Zhou, L.Y., El-Boubbou, K., Ye, X.S., Huang, X.F.: Multicomponent one-pot synthesis of the tumor-associated carbohydrate antigen Globo-H based on preactivation of thioglycosyl donors. J. Organomet. Chem. **72**, 6409–6420 (2007)
12. Ravida, A., Liu, X.Y., Kovacs, L., Seeberger, P.H.: Synthesis of glycosyl phosphates from 1,2-orthoesters and application to in situ glycosylation reactions. Org. Lett. **8**, 1815–1818 (2006)
13. Westheimer, F.H.: Why nature chose phosphates. Science. **235**, 1173–1178 (1987)
14. Denekamp, C., Sandlers, Y.: Anomeric distinction and oxonium ion formation in acetylated glycosides. J. Mass Spectrom. **40**, 765–771 (2005)
15. Denekamp, C., Sandlers, Y.: Formation and stability of oxocarbenium ions from glycosides. J. Mass Spectrom. **40**, 1055–1063 (2005)
16. O'Brien, P.J.: Catalytic promiscuity and the divergent evolution of DNA repair enzymes. Chem. Rev. **106**, 720–752 (2006)
17. Stivers, J.T., Jiang, Y.L.: A mechanistic perspective on the chemistry of DNA repair glycosylases. Chem. Rev. **103**, 2729–2759 (2003)
18. Kancharla, P.K., Navuluri, C., Crich, D.: Dissecting the influence of oxazolidinones and cyclic carbonates in sialic acid chemistry. Angew. Chem. Int. Ed. **51**, 11105–11109 (2012)
19. Splitter, J.S.: Applications of mass spectrometry to organic stereochemistry. VCH Publisher, New York (1994)
20. Dallinga, J.W., Heerma, W.: Reaction-mechanism and fragment ion structure determination of deprotonated small oligosaccharides, studied by negative-ion fast-atom-bombardment (tandem) mass-spectrometry. Biol. Mass Spectrom. **20**, 215–231 (1991)
21. Hofmeister, G.E., Zhou, Z., Leary, J.A.: Linkage position determination in lithium-cationized disaccharides: tandem mass spectrometry and semiempirical calculations. J. Am. Chem. Soc. **113**, 5964–5970 (1991)
22. Smith, G., Leary, J.A.: Differentiation of stereochemistry of glycosidic bond configuration: tandem mass spectrometry of diastereomeric cobalt-glucosyl-glucose disaccharide complexes. J. Am. Soc. Mass Spectrom. **7**, 953–957 (1996)
23. Dang, T.T., Pedersen, S.F., Leary, J.A.: Chiral recognition in the gas-phase: mass spectrometric studies of diastereomeric cobalt complexes. J. Am. Soc. Mass Spectrom. **5**, 452–459 (1994)
24. Jorge, T.F., Florencio, M.H., Ribeiro-Barros, A.I., Antonio, C.: Quantification and structural characterization of raffinose family oligosaccharides in Casuarina glauca plant tissues by porous graphitic carbon electrospray quadrupole ion trap mass spectrometry. Int. J. Mass Spectrom. **413**, 127–134 (2017)
25. Zaia, J., Costello, C.E.: Tandem mass spectrometry of sulfated heparin-like glycosaminoglycan oligosaccharides. Anal. Chem. **75**, 2445–2455 (2003)
26. Reis, A., Domingues, M.R.M., Domingues, P., Ferrer-Correia, A.J., Coimbra, M.A.: Positive and negative electrospray ionisation tandem mass spectrometry as a tool for structural characterisation of acid released oligosaccharides from olive pulp glucuronoxylans. Carbohydr. Res. **338**, 1497–1505 (2003)
27. Bae, J., Song, H., Moon, B., Oh, H.B.: Collisional activation dissociation mass spectrometry studies of oligosaccharides conjugated with Na^+-encapsulated dibenzo-18-crown-6 ether. Mass Spectrom. Lett. **7**, 96–101 (2016)
28. McLafferty, F.W.: Mass spectrometric analysis broad applicability to chemical research. Anal. Chem. **28**, 306–316 (1956)
29. Wuhrer, M., Deelder, A.M., van der Burgt, Y.E.M.: Mass spectrometric glycan rearrangements. Mass Spectrom. Rev. **30**, 664–680 (2011)
30. Grossert, J.S., Cook, M.C., White, R.L.: The influence of structural features on facile McLafferty-type, even-electron rearrangements in tandem mass spectra of carboxylate anions. Rapid Commun. Mass Spectrom. **20**, 1511–1516 (2006)
31. Chai, Y.F., Pan, Y.J.: The effect of cation size (H^+, Li^+, Na^+, and K^+) on McLafferty-type rearrangement of even-electron ions in mass spectrometry. Sci. China Chem. **57**, 662–668 (2014)
32. Tseng, K., Lindsay, L.L., Penn, S., Hedrick, J.L., Lebrilla, C.B.: Characterization of neutral oligosaccharide-alditols from *Xenopus laevis* egg jelly coats by matrix-assisted laser desorption Fourier transform mass spectrometry. Anal. Biochem. **250**, 18–28 (1997)
33. Ozcan, S., An, H.J., Vieira, A.C., Park, G.W., Kim, J.H., Mannis, M.J., Lebrilla, C.B.: Characterization of novel O-glycans isolated from tear and saliva of ocular rosacea patients. J. Proteome Res. **12**, 1090–1100 (2013)
34. An, H.J., Ninonuevo, M., Aguilan, J., Liu, H., Lebrilla, C.B., Alvarenga, L.S., Mannis, M.J.: Glycomics analyses of tear fluid for the diagnostic detection of ocular rosacea. J. Proteome Res. **4**, 1981–1987 (2005)
35. Harvey, D.J., Bateman, R.H., Green, M.R.: High-energy collision-induced fragmentation of complex oligosaccharides ionized by matrix-assisted laser desorption/ionization mass spectrometry. J. Mass Spectrom. **32**, 167–187 (1997)
36. De Winter, J., Coulembier, O., Dubois, P., Gerbaux, P.: Collision-induced dissociation of polymer ions: charge driven decomposition for sodium-cationized polylactides and isomeric end-group distinction. Int. J. Mass Spectrom. **308**, 11–17 (2011)
37. Laine, O., Laitinen, T., Vainiotalo, P.: Characterization of polyesters prepared from three different phthalic acid isomers by CID-ESI-FT-ICR and PSD-MALDI-TOF mass spectrometry. Anal. Chem. **74**, 4250–4258 (2002)
38. Lemoine, J., Fournet, B., Despeyroux, D., Jennings, K.R., Rosenberg, R., Dehoffmann, E.: Collision-induced dissociation of alkali-metal cationized and permethylated oligosaccharides: influence of the collision energy and of the collision gas for the assignment of linkage position. J. Am. Soc. Mass Spectrom. **4**, 197–203 (1993)
39. Yuan, H., Liu, L., Gu, J.P., Liu, Y., Fang, M.J., Zhao, Y.F.: Distinguishing isomeric aldohexose-ketohexose disaccharides by electrospray ionization mass spectrometry in positive mode. Rapid Commun. Mass Spectrom. **29**, 2167–2174 (2015)
40. Cancilla, M.T., Penn, S.G., Carroll, J.A., Lebrilla, C.B.: Coordination of alkali metals to oligosaccharides dictates fragmentation behavior in matrix assisted laser desorption ionization Fourier transform mass spectrometry. J. Am. Chem. Soc. **118**, 6736–6745 (1996)
41. Asam, M.R., Glish, G.L.: Tandem mass spectrometry of alkali cationized polysaccharides in a quadrupole ion trap. J. Am. Soc. Mass Spectrom. **8**, 987–995 (1997)
42. Xie, Y.M., Lebrilla, C.B.: Infrared multiphoton dissociation of alkali metal-coordinated oligosaccharides. Anal. Chem. **75**, 1590–1598 (2003)
43. Harvey, D.J.: Collision-induced fragmentation of underivatized N-linked carbohydrates ionized by electrospray. J. Mass Spectrom. **35**, 1178–1190 (2000)
44. Bylka, W., Franski, R., Stobiecki, M.: Differentiation between isomeric acacetin-6-C-(6"-O-malonyl)glucoside and acacetin-S-C-(6"-O-malonyl)glucoside by using low-energy CID mass spectra. J. Mass Spectrom. **37**, 648–650 (2002)
45. Tao, W.A., Wu, L.M., Cooks, R.G.: Differentiation and quantitation of isomeric dipeptides by low-energy dissociation of copper(II)-bound complexes. J. Am. Soc. Mass Spectrom. **12**, 490–496 (2001)
46. Hoffmann, W., Hofmann, J., Pagel, K.: Energy-resolved ion mobility-mass spectrometry: A concept to improve the separation of isomeric carbohydrates. J. Am. Soc. Mass Spectrom. **25**, 471–479 (2014)

47. March, R.E.: Quadrupole ion trap mass spectrometry: a view at the turn of the century. Int. J. Mass Spectrom. **200**, 285–312 (2000)
48. Kenttamaa, H.I., Cooks, R.G.: Internal energy distributions acquired through collisional activation at low and high energies. Int. J. Mass Spectrom. Ion Process. **64**, 79–83 (1985)
49. Kertesz, T.M., Hall, L.H., Hill, D.W., Grant, D.F.: CE50: quantifying collision induced dissociation energy for small molecule characterization and identification. J. Am. Soc. Mass Spectrom. **20**, 1759–1767 (2009)
50. Kuki, A., Nagy, L., Memboeuf, A., Drahos, L., Vekey, K., Zsuga, M., Keki, S.: Energy-dependent collision-induced dissociation of lithiated polytetrahydrofuran: effect of the size on the fragmentation properties. J. Am. Soc. Mass Spectrom. **21**, 1753–1761 (2010)
51. Sleno, L., Volmer, D.A.: Ion activation methods for tandem mass spectrometry. J. Mass Spectrom. **39**, 1091–1112 (2004)
52. Danikiewicz, W., Tarnowski, P., Bienkowski, T., Jurczak, J.: Estimation of the noncovalent bond dissociation energies of the gas-phase complexes of macrocyclic polyethers with alkali metal cations using an electrospray ionization/triple quadrupole mass spectrometer. Pol. J. Chem. **78**, 699–709 (2004)
53. Rosu, F., Nguyen, C.H., De Pauw, E., Gabelica, V.: Ligand binding mode to duplex and triplex DNA assessed by combining electrospray tandem mass spectrometry and molecular modeling. J. Am. Soc. Mass Spectrom. **18**, 1052–1062 (2007)
54. Zhu, Y., Hamlow, L.A., He, C.C., Strobehn, S.F., Lee, J.K., Gao, J., Berden, G., Oomens, J., Rodgers, M.T.: Influence of sodium cationization versus protonation on the gas-phase conformations and glycosidic bond stabilities of 2'-deoxyadenosine and adenosine. J. Phys. Chem. B. **120**, 8892–8904 (2016)
55. Zhu, Y., Hamlow, L.A., He, C.C., Lee, J.K., Gao, J., Berden, G., Oomens, J., Rodgers, M.T.: Gas-phase conformations and N-glycosidic bond stabilities of sodium caionized 2'-deoxyguanosine and guanosine: sodium cations preferentially bind to the guanine residue. J. Phys. Chem. B. **121**, 4048–4060 (2017)
56. Zhu, Y., Hamlow, L.A., He, C.C., Roy, H.A., Cunningham, N.A., Munshi, M.U., Berden, G., Oomens, J., Rodgers, M.T.: Conformations and N-glycosidic bond stabilities of sodium cationized 2'-deoxycytidine and cytidine: Solution conformation of $[Cyd+Na]^+$ is preserved upon ESI. Int. J. Mass Spectrom. in press. (2017). https://doi.org/10.1016/j.ijms.2017.04.005
57. Zhu, Y., Roy, H.A., Cunningham, N.A., Strobehn, S.F., Gao, J., Munshi, M.U., Berden, G., Oomens, J., Rodgers, M.T.: Effects of sodium cationization versus protonation on the conformations and N-glycosidic bond stabilities of sodium cationized uridine and 2'-deoxyuridine: solution conformation of $[Urd+Na]^+$ is preserved upon ESI. Phys. Chem. Chem. Phys. **19**, 17637-17652 (2017)
58. Zhu, Y., Roy, H.A., Cunningham, N.A., Strobehn, S.F., Gao, J., Munshi, M.U., Berden, G., Oomens, J., Rodgers, M.T.: IRMPD action spectroscopy, ER-CID experiments, and theoretical studies of sodium cationized thymidine and 5-methyluridine: kinetic trapping during the ESI desolvation process preserves the solution structure of $[Thd+Na]^+$. J. Am. Soc. Mass Spectrom. ín press (2017). https://doi.org/10.1007/s13361-017-1753-5
59. Bovet, C., Wortmann, A., Eiler, S., Granger, F., Ruff, M., Gerrits, B., Moras, D., Zenobi, R.: Estrogen receptor-ligand complexes measured by chip-based nanoelectrospray mass spectrometry: an approach for the screening of endocrine disruptors. Protein Sci. **16**, 938–946 (2007)
60. Rosu, F., Pirotte, S., De Pauw, E., Gabelica, V.: Positive and negative ion mode ESI-MS and MS/MS for studying drug-DNA complexes. Int. J. Mass Spectrom. **253**, 156–171 (2006)
61. Crich, D., Sun, S.X.: Direct chemical synthesis of beta-mannopyranosides and other glycosides via glycosyl triflates. Tetrahedron. **54**, 8321–8348 (1998)
62. Crich, D., Dudkin, V.: Efficient, diastereoselective chemical synthesis of a beta-mannopyranosyl phosphoisoprenoid. Org. Lett. **2**, 3941–3943 (2000)
63. Crich, D.: Mechanism of a chemical glycosylation reaction. Acc. Chem. Res. **43**, 1144–1153 (2010)
64. Crich, D., Vinogradova, O.: On the influence of the C2–O2 and C3–O3 bonds in 4,6-O-benzylidene-directed beta-mannopyranosylation and alpha-glucopyranosylation. J. Organomet. Chem. **71**, 8473–8480 (2006)
65. Memboeuf, A., Nasioudis, A., Indelicato, S., Pollreisz, F., Kuki, A., Keki, S., van den Brink, O.F., Vekey, K., Drahos, L.: Size effect on fragmentation in tandem mass spectrometry. Anal. Chem. **82**, 2294–2302 (2010)
66. Memboeuf, A., Jullien, L., Lartia, R., Brasme, B., Gimbert, Y.: Tandem mass spectrometric analysis of a mixture of isobars using the survival yield technique. J. Am. Soc. Mass Spectrom. **22**, 1744–1752 (2011)
67. Derwa, F., Depauw, E., Natalis, P.: New basis for a method for the estimation of secondary ion internal energy-distribution in soft ionization techniques. Org. Mass Spectrom. **26**, 117–118 (1991)
68. Guo, X.H., Duursma, M.C., Kistemaker, P.G., Nibbering, N.M.M., Vekey, K., Drahos, L., Heeren, R.M.A.: Manipulating internal energy of protonated biomolecules in electrospray ionization Fourier transform ion cyclotron resonance mass spectrometry. J. Mass Spectrom. **38**, 597–606 (2003)
69. Yassaghi, G., Jasikova, L., Roithova, J.: Gas-phase study of metal complexes with redox-active ligands. Int. J. Mass Spectrom. **407**, 92–100 (2016)
70. Alahmadi, Y.J., Gholami, A., Fridgen, T.D.: The protonated and sodiated dimers of proline studied by IRMPD spectroscopy in the N-H and O-H stretching region and computational methods. Phys. Chem. Chem. Phys. **16**, 26855–26863 (2014)
71. Rodgers, M.T., Armentrout, P.B.: Noncovalent metal–ligand bond energies as studied by threshold collision-induced dissociation. Mass Spectrom. Rev. **19**, 215–247 (2000)
72. Armentrout, P.B., Rodgers, M.T.: An absolute sodium cation affinity scale: threshold collision-induced dissociation experiments and ab initio theory. J. Phys. Chem. A. **104**, 2238–2247 (2000)
73. Fales, B.S., Fujamade, N.O., Oomens, J., Rodgers, M.T.: Infrared multiple photon dissociation action spectroscopy and theoretical studies of triethyl phosphate complexes: effects of protonation and sodium cationization on structure. J. Am. Soc. Mass Spectrom. **22**, 1862–1871 (2011)
74. Polfer, N.C., Oomens, J., Dunbar, R.C.: Alkali metal complexes of the dipeptides PheAla and AlaPhe: IRMPD spectroscopy. ChemPhysChem. **9**, 579–589 (2008)
75. Ruan, C.H., Rodgers, M.T.: Cation-pi interactions: structures and energetics of complexation of Na^+ and K^+ with the aromatic amino acids, phenylalanine, tyrosine, and tryptophan. J. Am. Chem. Soc. **126**, 14600–14610 (2004)
76. Amunugama, R., Rodgers, M.T.: Influence of substituents on cation–pi interactions. 1. Absolute binding energies of alkali metal cation–toluene complexes determined by threshold collision-induced dissociation and theoretical studies. J. Phys. Chem. A. **106**, 5529–5539 (2002)
77. Amunugama, R., Rodgers, M.T.: Influence of substituents on cation-pi interactions. 2. Absolute binding energies of alkali metal cation–fluorobenzene complexes determined by threshold collision-induced dissociation and theoretical studies. J. Phys. Chem. A. **106**, 9092–9103 (2002)
78. Amunugama, R., Rodgers, M.T.: Influence of substituents on cation-pi interactions. 3. Absolute binding energies of alkali metal cation-aniline complexes determined by threshold collision-induced dissociation and theoretical studies. Int. J. Mass Spectrom. **227**, 339–360 (2003)
79. Amunugama, R., Rodgers, M.T.: The influence of substituents on cation–pi interactions. 4. Absolute binding energies of alkali metal cation – phenol complexes determined by threshold collision-induced dissociation and theoretical studies. J. Phys. Chem. A. **106**, 9718–9728 (2002)
80. Amunugama, R., Rodgers, M.T.: Influence of substituents on cation–pi interactions. 5. Absolute binding energies of alkali metal cation-anisole complexes determined by threshold collision-induced dissociation and theoretical studies. Int. J. Mass Spectrom. **222**, 431–450 (2003)
81. Kadentsev, V.I., Kaymarazov, A.G., Chizhov, O.S., Cerny, M., Trnka, T., Turecek, F.: Mass spectra of 1,6:2,3- and 1,6:3,4-dianhydro- beta-D-hexopyranose derivatives: formation of cluster ions assisted by participation of neighboring acyloxy groups. Biomed. Mass Spectrom. **9**, 130–134 (1982)
82. Kuzmenkov, I., Etinger, A., Mandelbaum, A.: Role of hydrogen migration in the mechanism of acetic acid elimination from MH^+ ions of acetates on chemical ionization and collision-induced dissociation. J. Mass Spectrom. **34**, 797–803 (1999)